

Chapter 18

Data-Driven Evolutionary-Game-Based Control for Drinking-Water Networks

Julián Barreiro-Gomez, Gerardo Riaño-Briceño, Carlos Ocampo-Martínez and Nicanor Quijano

18.1 Introduction

Around 663 million people had no access to safe drinking water in 2015, and around 2.4 billion people live without adequate sanitation according to [25]. This situation has impacts on the economy of the society according to the Millennium Summit of 2000, on which the United Nations agreed the Millennium Development Goals (MDG). One of the biggest concerns of the MDG, due to the rapid population growth and industrialization, is to guarantee the access to drinking water, achieving a proper management of the available water resources. Hence, it becomes essential to overcome the lack of drinking water for achieving sustainable development including in both social and economic aspects, poverty reduction and equity, and also sustainable environmental services [13].

Over the last decade, several optimization-based control strategies have been proposed to manage efficiently drinking water and to solve resource allocation problems in water applications. For instance, in [10] a nonlinear multi-objective optimization procedure has been proposed to manage water flows and reserves in drinking water transport networks (DWTNs), considering the uncertainty of climate and global change development, using an integrated approach, i.e., modelling the drinking-water system, the climate, and the society as a whole. However, this solution implies to consider a lot of variables and constraints which increase the complexity of the optimization problem. Likewise, optimization-based strategies such as model predictive

J. Barreiro-Gomez · C. Ocampo-Martínez (✉)
Institut de Robòtica i Informàtica Industrial, CSIC-UPC, Barcelona, Spain
e-mail: cocampo@iri.upc.edu

G. Riaño-Briceño · N. Quijano
Departamento de Ingeniería Eléctrica y Electrónica, Universidad de los Andes, Bogotá, Colombia

© Springer International Publishing AG 2017
V. Puig et al. (eds.), *Real-Time Monitoring and Operational Control of Drinking-Water Systems*, Advances in Industrial Control,
DOI 10.1007/978-3-319-50751-4_18

363

control (MPC) have been designed for this kind of systems, considering the uncertainty of demand patterns as in [26] and minimizing operational costs and shortage events [9].

Another approach to address the DWTN control design is the use of population dynamics taking advantage of their stability properties and the close relationship between the solution in a population game (Nash equilibrium) and the unique maximizer of a constrained convex optimization problem [23]. Recently, game theory has been used in the solution of engineering problems [1, 14, 17, 24] and for the solution of optimization problems [15, 16]. Furthermore, in this chapter, the population game approach is presented as a powerful tool for the design of data-driven controllers. More precisely, two different directions in the design of data-driven population-games-based controllers are treated in this work. First, the DWTN is controlled by making a partitioning into subsystems that satisfy specific conditions, and a resource allocation problem is solved at each partition. This approach generates a decentralized control scheme since the local controllers neither communicate to each other nor exchange information among them. Secondly, it is proposed the design of data-driven controllers by minimizing a cost function and considering flow-balance constraints. Under this approach, the network is divided into subsystems according to the established constraints over the control inputs, which constitutes a distributed scheme due to the existing intersection among the different subsystems.

The presented contents in this chapter are a compilation of the theory proposed in previous works [3–6, 21]. However, some new case studies are incorporated as well as new simulation results.

Notation

Although this book follows an unified notation and in order to facilitate the reading of this chapter, some additional notation is introduced. The subindex is associated to a node of a graph or to a strategy in a game. On the other hand, the superindex refers to a population. For instance, the subindex i in u_i , \mathcal{P}_i , u_i^p or f_i refers either to a node in a graph or to a strategy, and the superindex p in m^p , \mathbf{u}^p , u_i^p or n^p indicates a population. Also it should be clear that the superindex is not an operational number, i.e., n^3 refers to population three but $n^3 \neq nnn$. We use bold font for column vectors and matrices, e.g., \mathbf{u} , and \mathbf{H} ; and non-bold style is used for scalar numbers, e.g., n^p . Calligraphy style is used for sets, e.g., \mathcal{S} . The column vector with n unitary entries is denoted by $\mathbf{1}_n$, and the column vector with null entries and suitable dimension is denoted by $\mathbf{0}$. The identity matrix with dimension $n \times n$ is denoted by \mathbb{I}_n . The cardinality of a set \mathcal{S} is denoted by $|\mathcal{S}|$. The continuous time is denoted by t , and it is mostly omitted throughout the manuscript in order to simplify the notation. Finally, $\mathbb{R}_{\geq 0}$ represents the set of all non-negative real numbers, and $\mathbb{Z}_{>0}$ represents the set of positive integer numbers.

18.2 Problem Statement

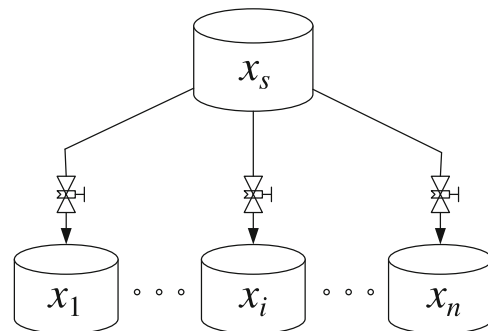
18.2.1 First Data-Driven Perspective

In the proposed DWTN model for the design of the population dynamics-based controllers, which is composed by several storage tanks, the flow direction is unique since it is assumed that the pressure head at upstream tanks of the network is always higher than the pressure head at downstream tanks. This consideration is common in DWTNs that have been designed for places where the topography is steep and the slope is descending. Due to this assumption, it is possible to distinguish between source and receptor tanks, taking into account that the former ones are always upstream and directly linked to the latter ones.

Consider then a simple DWTN composed by n receptor tanks, and only one source tank as shown in Fig. 18.1. This topology is known as *branched* [19], which means that there are no loops in the network due to the fact that several outflows might go out from a single source tank, but no several inflows come into a single receptor. Let $\mathcal{S} = \{1, \dots, n\}$ be the set of receptor tanks in the *branched* subsystem. The volume of the tank $i \in \mathcal{S}$ is denoted by $x_i \in \mathbb{R}_{\geq 0}$, its maximum volume is denoted by $x_i^{\max} \in \mathbb{R}_{\geq 0}$ and its inflows and outflows are given by $q_i^{\text{in}} \in \mathbb{R}_{\geq 0}$ and $q_i^{\text{out}} \in \mathbb{R}_{\geq 0}$, respectively. Hence, the vector of all the tank volumes is denoted $\mathbf{x} \in \mathbb{R}_{\geq 0}^n$, and the vector of maximum volumes is $\mathbf{x}^{\max} \in \mathbb{R}_{\geq 0}^n$. The parameter $u_i \in [0, 1]$ determines the setting of the input valve in the i th tank, $K_i > 0$ scales the outflow, and it can be considered as a volume-flow conversion factor or the discharge coefficient of the tank. Moreover, the system is affected by perturbations that are related to daily demand patterns.

The control objective consists in avoiding shortages throughout the system, i.e., to avoid that the current volume of the tank x_i runs out, not supplying the demand, for all $i \in \mathcal{S}$. To achieve this objective, it is proposed to do an allocation of the available resource stored in the n tanks, i.e., to distribute the current available volume given by $x_i^{\max} - x_i$ in an optimal way by controlling the inflows q_i^{in} , for all $i \in \mathcal{S}$. For instance, considering the hypothetical situation in which one tank is completely filled and another tank is empty, more priority should be assigned to the inflow of the empty tank rather than the inflow assigned to the filled one, in order to prevent shortages.

Fig. 18.1 Branched topology with n receptor tanks, and one source tank whose volume is denoted by v_s . The source tank is upstream of the receptor tanks



For each subsystem, the topology of interest is given by different receptor tanks and one source. The entire control system for the DWTN is composed by π local controllers that do not communicate with each other and which operate independently in parallel, i.e., all local controllers may operate their corresponding control inputs at once.

18.2.2 Second Data-Driven Perspective

This section presents the design of a controller without considering the model of the system, but just by considering the fact that the error within a tank (i.e., the difference between the safety value and the current volume) can be reduced as the control action is increased. In order to design a data-driven controller based on the proposed methodology, it is defined a cost function corresponding to the desired behaviour of the system. In this particular case, a volume error at each tank is considered.

The controller is designed through an optimization problem minimizing economical costs, the volume error with respect to the safety storage term and variations in the control actions. The economical costs are given by $(\alpha_1^p + \alpha_2^p(k))^\top \mathbf{u}^p(k)$, where α_1^p is a constant vector defining the energy costs, and α_2^p is a time varying vector determining the water costs. The volume error is given by $\mathbf{x}_s^p - \mathbf{x}^p$, where \mathbf{x}_s^p is the safety storage imposed by the company in charge of the system management. Finally, the $\Delta \mathbf{u}^p(k)^\top \Delta \mathbf{u}^p(k)$ corresponds to the smooth operation cost.

These objectives are minimized subject to constraints of mass balance and physical constraints of actuators. To this end, new variables $\tilde{\mathbf{x}}_s \in \mathbb{R}^{n_u}$ of safety values, and $\tilde{\mathbf{x}} \in \mathbb{R}^{n_u}$ composed of tank volumes, are introduced. Notice that the dimension of the new vectors of volumes corresponds to the dimension of the vector of control actions, i.e., $\tilde{\mathbf{x}}_s, \tilde{\mathbf{x}}, \mathbf{u} \in \mathbb{R}^{n_u}$. The scalar \tilde{x}_i denotes the volume corresponding to the tank whose inflow is given by u_i , and null in case that u_i is not an inflow for any tank. The safety volume $\tilde{x}_{s,i}$ corresponds to the safety volume of the tank whose inflow is given by u_i , and null otherwise. Briefly, $\tilde{x}_i = x_j$, and $\tilde{x}_{s,i} = x_{s,j}$ if u_i is the inflow of the j th tank, and null if u_i is not an inflow for any tank. Notice that the constraints over the system states (i.e., tanks volumes) may not be considered since this approach does not use a Control-Oriented Model (COM). The following optimization problem only depends on measured state values (volumes) and decision variables (control inputs):

$$\begin{aligned}
 & \underset{\mathbf{u}^p}{\text{maximize}} \quad V(\mathbf{u}^p(k)) = -\gamma_1(\alpha_1^p + \alpha_2^p(k))^\top \mathbf{u}^p(k) \\
 & \quad -\gamma_2(\tilde{\mathbf{x}}_s^p - \tilde{\mathbf{x}}^p(k))^\top \text{diag}(\mathbf{u}^p(k)) (\tilde{\mathbf{x}}_s^p - \tilde{\mathbf{x}}^p(k)) - \gamma_3 \Delta \mathbf{u}^p(k)^\top \Delta \mathbf{u}^p(k), \\
 & \text{subject to} \quad \mathbf{E}_u^p \mathbf{u}^p(k) = -\mathbf{E}_d^p \mathbf{d}^p(k), \\
 & \quad \begin{bmatrix} \mathbb{I}_{n_u} \\ -\mathbb{I}_{n_u} \end{bmatrix} \mathbf{u}^p(k) \leq \begin{bmatrix} \mathbf{u}^{p,\max} \\ -\mathbf{u}^{p,\min} \end{bmatrix}.
 \end{aligned} \tag{18.1}$$

18.3 Proposed Approach

18.3.1 Population-Games Approach: First Data-Driven Perspective

In this section, a detailed description of the population dynamics-based controller is done, taking into consideration that it is presented for the case of a single partition or subsystem. As it was stated before, the control approach is conceived from an analogy between the population dynamics framework and the DWTN model (see Table 18.1). In order to make clearer the analogy, it is worth to understand the process of transport between a source tank and the final user.

First of all, storage tanks receive water from treatment plants and/or natural water bodies (e.g., aquifers and reservoirs). Then, this water is redistributed among several storage tanks, which are located close to the final user. For instance, these can be placed in houses to prevent shortage when there is a lack of the resource. Consumers use the water that is available for them into the closest tank. In order to match supply and demand, the utility has the possibility to manipulate the amount of water that is deposited into receptor tanks through valves.

Considering this process, one can notice that the control problem is reduced to a resource allocation problem, in which the system can be seen as the population of a game. The population is composed by water or flow units, which summed all up form a mass (outflow). When the population mass reaches a point in which the flow diverges, it has the possibility to select one of the n paths (strategies) that lead to one of the receptor tanks in \mathcal{S} . The mass is going to select certain strategy based on the maximization of its wealth, which is defined by a fitness function.

Now that the analogy has been exposed, consider the branched DWTN with $n \in \mathbb{Z}_{>0}$ receptor tanks (strategies). The total flow through the system (population mass) is denoted by $Q \in \mathbb{R}_{>0}$, which corresponds to the outflow of the source tank. Each flow unit is assigned to an inflow of one of the receptor tanks.

The scalar $u_i \in \mathbb{R}_{\geq 0}$ is the proportion of flow units assigned to each flow associated to the tank $i \in \mathcal{S}$ as a percentage, i.e., the inflow for the i th tank is given by $u_i Q$. The

Table 18.1 Equivalence between population dynamics and DWTN

	Population dynamics	DWTN
\mathcal{P}	Population	System
i	Strategy	Receptor tanks
m	Population mass	Total outflow source tank
q	Agents	Flow units
u_i	Proportion of agents	Proportion of flow
\mathbf{u}	Strategic distribution	Flow distribution in receptor tanks
f_i	Fitness of a strategy	Available volume capacity

vector $\mathbf{u} \in \mathbb{R}_{\geq 0}^n$ is the flow proportion distribution involving the n tanks according to the topology. The set of the possible distributions of flow is given by a simplex

$$\Delta = \left\{ \mathbf{u} \in \mathbb{R}_{\geq 0}^n : \sum_{i \in \mathcal{S}} u_i = 1 \right\},$$

and the tangent space of the set of possible distributions of flow is defined as

$$T\Delta = \left\{ \mathbf{z} \in \mathbb{R}^n : \sum_{i \in \mathcal{S}} z_i = 0 \right\}.$$

Each flow unit is assigned to each tank $i \in \mathcal{S}$ depending on the current volume capacity, which is described by a function $f_i(\mathbf{u})$. Therefore, less inflow is assigned to those tanks close to be filled up.

The design of the population dynamics-based controllers are given by the proper selection of the fitness functions that define the incentives for the proportion of agents to choose a particular strategy. The proper selection of the fitness functions is further discussed below, and it depends on how the water is distributed in a DWTN with branched topology. Furthermore, it is necessary that the fitness functions satisfy conditions to obtain a class of population game known as stable game [11].

Definition 18.1 The game $\mathbf{F}(\mathbf{u})$ is stable if the Jacobian matrix $\mathbf{J} = \mathbf{D}\mathbf{F}(\mathbf{u})$ is negative semi-definite with respect to the tangent space $T\Delta$ [11], i.e.,

$$\mathbf{z}^\top \mathbf{J} \mathbf{z} \leq 0, \text{ for all } \mathbf{z} \in T\Delta, \mathbf{u} \in \Delta.$$

Then, it implies that a game is stable if the fitness functions are decreasing with respect to the proportion of agents.

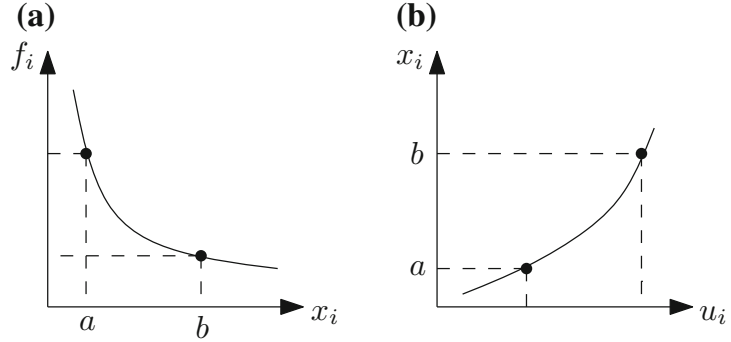
Notice that for the branched topology, the fitness functions can be selected decreasing with respect to the current volume, e.g., the error with respect to the maximum capacity volume as in [20] (see Fig. 18.2a). When a proportion of agents is increased, it is expected that the corresponding volume increases (see Fig. 18.2b). Consequently, due to the fact that fitness functions are increasing with respect to the volume, the fitness function decreases with respect to the proportion of agents (necessary condition for a stable game).

The Distributed Replicator Dynamics

The results presented on this chapter are obtained using the replicator dynamics [23] in order to find a solution to the resource allocation problem. The solution, in which no agent has incentives to switch from one strategy to another one [23], is determined in terms of a *Nash equilibrium*,¹ which can be found when the dynamics converge,

¹ $\mathbf{u}^* \in \Delta$ is a Nash equilibrium if each used strategy entails the maximum benefit for the proportion of agents selecting it, i.e., the set of Nash equilibria is given by $\{\mathbf{u}^* \in \Delta : u_i^* > 0 \Rightarrow f_i(\mathbf{u}^*) \geq f_j(\mathbf{u}^*)\}$, for all $i, j \in \mathcal{S}$ [23].

Fig. 18.2 Proper selection of fitness functions for divergence topology (a) and (b). Correspondence is as follows: **a** decreasing fitness function with respect to volume. **b** increasing relation existing between proportion of agents and volume for divergence topology



and is denoted by $\mathbf{u}^* \in \Delta$. The replicator dynamics are of interest in this work since they share gradient properties studied in [22], and because of their passivity properties studied in [3]. However, the replicator dynamics require full information (i.e., all the tanks (strategies) need information about the states of the others in order to evolve).

Since the problem is handled using a distributed control approach, it is necessary to use the distributed replicator dynamics, which were deduced in [2] from a local revision protocol that only needs partial information. Due to the fact that only local information is needed, then there is an undirected non-complete connected graph describing the interactions among agents. It is denoted by $\mathcal{G} = (\mathcal{V}, \mathcal{E})$, where \mathcal{V} is the set of nodes, which represents the tanks, and $\mathcal{E} \subset \{(i, j) : i, j \in \mathcal{V}\}$ is the set of links representing the information sharing within the system. Furthermore, the set of neighbours of the node $i \in \mathcal{V}$ is given by $\mathcal{N}_i = \{j : (i, j) \in \mathcal{E}\}$. Notice that $i \notin \mathcal{N}_i$, and that $\mathcal{N}_i \neq \emptyset$, for all $i \in \mathcal{V}$ since \mathcal{G} is connected.

The distributed replicator dynamics are given by

$$\dot{u}_i = u_i \left(f_i(\mathbf{u}) \sum_{j \in \mathcal{N}_i} u_j - \sum_{j \in \mathcal{N}_i} u_j f_j(\mathbf{u}) \right), \quad \text{for all } i \in \mathcal{S}.$$

Now that the distributed replicator dynamics have been defined, consider a population composed by a large and finite number of agents. Agents in the population have incentives to select the tank outflows (e.g., in a general control system, the error is an incentive for the controller to apply more energy to the system and then correct the states to achieve the desired values). The incentives, associated to rewarding that the proportion of agents u_i receives, for selecting the tank $i \in \mathcal{S}$, are given by a fitness function $f_i(\mathbf{u})$ whose mapping is $f_i : \Delta \mapsto \mathbb{R}$. Moreover, the vector of all the fitness functions is denoted by $\mathbf{F} = [f_1 \ \cdots \ f_n]^\top$ with mapping $\mathbf{F} : \Delta \mapsto \mathbb{R}^n$.

The solution of the population game is given by the condition $f_i = f_j$, for all $i, j \in \mathcal{S}$. In order to control the *case of flow divergence* topology, it is proposed the following fitness function

$$f_i = - \left(\frac{1}{e_i + \varepsilon} \right), \quad \text{for all } i \in \mathcal{S}, \quad (18.2)$$

with

$$e_i = 1 - \frac{x_i + s_i + \gamma}{x_i^{\max} + \gamma}, \quad \text{for all } i \in \mathcal{S},$$

where $s_i \in \mathbb{R}_{\geq 0}$ is the shortage volume, i.e., the volume that is demanded but cannot be supplied by the i th tank, $\gamma \in \mathbb{R}_{> 0}$ is a constant that ensures $0 \leq e_i \leq 1$ and $\varepsilon \in \mathbb{R}_{> 0}$ is a small factor that prevents the indetermination of f_i when $e_i = 0$. Moreover, the proposed fitness function for the strategy $i \in \mathcal{S}$, only depends on the volume v_i and the proportion of agents u_i , making it suitable to apply in this case where only local information is available.

All the valves, defining the inflow of the receptor tanks in a partition, are established by the vector $\mathbf{u} \in \mathbb{R}_{\geq 0}^n$. These settings in the output gates affect the behaviour of the tank volumes, i.e., $\mathbf{x} \in \mathbb{R}_{\geq 0}^n$. Then, the variation of the tank volumes modifies the fitness function (18.2), affecting the control actions over the output valves $\mathbf{u} \in \mathbb{R}_{\geq 0}^n$.

18.3.2 Population-Games Approach: Second Data-Driven Perspective

Consider a society whose topology is represented by an undirected non-complete connected graph denoted by $\mathcal{G} = (\mathcal{V}, \mathcal{E})$, where \mathcal{V} denotes the set of nodes of the graph \mathcal{G} . These nodes represent the set of n available strategies in a social game denoted by $\mathcal{S} = \{1, \dots, n\}$. Besides, the set $\mathcal{E} \subset \{(i, j) : i, j \in \mathcal{V}\}$ denotes the edges of the graph \mathcal{G} that determines the possible interactions among social strategies.

The graph \mathcal{G} is divided into $\pi \in \mathbb{Z}_{> 0}$ subcomplete graphs known as cliques [7]. Additionally, each clique represents a population within the society. The set $\mathcal{P} = \{1, \dots, \pi\}$ denotes the collection of the π populations, and the set of cliques is denoted by $\mathcal{C} = \{\mathcal{C}^p : p \in \mathcal{P}\}$. The clique corresponding to the population $p \in \mathcal{P}$ is a graph given by $\mathcal{C}^p = (\mathcal{V}^p, \mathcal{E}^p)$, where the set \mathcal{V}^p represents the n^p available strategies in a population game, which are denoted by $\mathcal{S}^p = \{i : i \in \mathcal{V}^p\}$. On the other hand, $\mathcal{E}^p = \{(i, j) : i, j \in \mathcal{V}^p\}$ is the set of all the possible links in \mathcal{C}^p determining full interaction among the population strategies.

In this work, it is assumed that the set of cliques is already known, i.e., the number of cliques π , the set of vertices \mathcal{V}^p and the set of edges \mathcal{E}^p for all $p \in \mathcal{P}$ are known. Although if it is desired to obtain the optimal set of cliques,² there are several methods to find them, e.g., the Bron Kerbosh algorithm [12], or the maximum clique problem using replicator dynamics as shown in [7]. Once the optimal set of cliques \mathcal{C} has been identified, it is possible to find *redundant links*. A link $(i, j) \in \mathcal{E}$ is redundant if $(i, j) \notin \tilde{\mathcal{E}}$, i.e., $(i, j) \notin \mathcal{E}^p$, for all $p \in \mathcal{P}$.

²The minimum amount of cliques π such that $\bigcup_{p \in \mathcal{P}} \mathcal{V}^p = \mathcal{V}$, and the minimum amount of links $|\tilde{\mathcal{E}}|$, where $\tilde{\mathcal{E}} = \bigcup_{p \in \mathcal{P}} \mathcal{E}^p \subseteq \mathcal{E}$ such that the graph $\tilde{\mathcal{G}} = (\mathcal{V}, \tilde{\mathcal{E}})$ is connected.

Then, the number of cliques that contain a node $i \in \mathcal{V}$, denoted by $G(i)$, is defined as follows:

$$G(i) = \sum_{p \in \mathcal{P}} g(i, p),$$

and

$$g(i, p) = \begin{cases} 1 & \text{if } i \in \mathcal{V}^p \\ 0 & \text{otherwise.} \end{cases}$$

Due to the fact that the graph \mathcal{G} is a non-complete and connected, then all cliques share at least one node with another clique, which is known as an intersection node. The set $\mathcal{I}^p = \{i \in \mathcal{V}^p : G(i) > 1\}$ collects all the intersection nodes in a population $p \in \mathcal{P}$. Moreover, the set of intersection nodes in the graph \mathcal{G} is given by $\mathcal{I} = \bigcup_{p \in \mathcal{P}} \mathcal{I}^p$.

Furthermore, all the populations $p \in \mathcal{P}$ such that a node $i \in \mathcal{V}$ belongs to the set of nodes \mathcal{V}^p are collected in a set denoted by \mathcal{P}_i . The set of all the populations that includes a node $i \in \mathcal{V}$ is given by $\mathcal{P}_i = \{p : i \in \mathcal{V}^p\}$, where $\mathcal{P}_i \subseteq \mathcal{P}$.

The scalar $u_i \in \mathbb{R}_{\geq 0}$ is the proportion of agents in the society selecting the strategy $i \in \mathcal{S}$. Similarly, the scalar $u_i^p \in \mathbb{R}_{\geq 0}$ is the proportion of agents selecting the strategy $i \in \mathcal{S}^p$ in the population $p \in \mathcal{P}$. Moreover, the distribution of agents throughout the available strategies in the society and populations is known as the social strategic distribution and the population strategic distribution denoted by $\mathbf{u} \in \mathbb{R}_{\geq 0}^n$ and $\mathbf{u}^p \in \mathbb{R}_{\geq 0}^{n^p}$, respectively.

The set of possible social strategic distributions is given by a simplex denoted by Δ , which is a constant set, i.e., $\Delta = \{\mathbf{u} \in \mathbb{R}_{\geq 0}^n : \sum_{i \in \mathcal{S}} u_i = m\}$, where $m \in \mathbb{R}_{> 0}$ is the constant mass of agents in the society. Similarly, the set of possible strategic distributions of the population $p \in \mathcal{P}$ is given by a non-constant simplex defined as $\Delta^p = \{\mathbf{u}^p \in \mathbb{R}_{\geq 0}^{n^p} : \sum_{i \in \mathcal{S}^p} u_i^p = m^p\}$, where $m^p \in \mathbb{R}_{> 0}$ corresponds to the mass of agents in the population $p \in \mathcal{P}$. Furthermore, there is a relationship between the social proportions and the population proportions given by

$$u_i = \frac{1}{G(i)} \sum_{p \in \mathcal{P}_i} u_i^p. \quad (18.3)$$

Notice that if it is considered that $u_i^p = 0$ for all $i \notin \mathcal{V}^p$, then (18.3) can be written as

$$u_i = \frac{1}{G(i)} \sum_{p \in \mathcal{P}} u_i^p. \quad (18.4)$$

The fitness functions take a social or population strategic distribution and return the payoff that a proportion of agents playing a certain strategy receives. Let $f_i : \Delta \mapsto \mathbb{R}$ be the mapping of the fitness function for the proportion of agents playing the strategy $i \in \mathcal{S}$, and $f_i^p : \Delta^p \mapsto \mathbb{R}$ be the mapping of the fitness function for the proportion of agents playing the strategy $i \in \mathcal{S}^p$ in the population $p \in \mathcal{P}$. The fitness corresponding

to a strategy $i \in \mathcal{S}$ is the same as the fitness for a strategy $j \in \mathcal{S}^p$ for all $p \in \mathcal{P}$ if $i = j$. Consequently, for all $i \in \mathcal{S}^p$ and for all $p \in \mathcal{P}_i$,

$$f_i(\mathbf{u}) = f_i^p(\mathbf{u}^p), \quad \text{if } u_i = u_i^p. \quad (18.5)$$

The vector of the fitness functions for a society is given by $\mathbf{F} = [f_1 \ \dots \ f_n]^\top \in \mathbb{R}^n$. The social average fitness is denoted by \bar{f} , where $\bar{f} = (\mathbf{u}^\top \mathbf{F})/m$. Similarly, the vector of fitness functions for a population $p \in \mathcal{P}$ is given by $\mathbf{F}^p \in \mathbb{R}^{n^p}$, whose fitness functions are associated to the strategies \mathcal{S}^p . The average fitness for a population $p \in \mathcal{P}$ is denoted by $\bar{f}^p = (\mathbf{u}^{p^\top} \mathbf{F}^p)/m^p$. There is a relationship between the population masses and the social mass given by

$$m = \sum_{p \in \mathcal{P}} m^p - \sum_{i \in \mathcal{S}} (G(i) - 1)u_i. \quad (18.6)$$

The framework of this paper is given by the assumptions stated next.

Assumption 18.1 The game \mathbf{F} is a full potential game [23], i.e., there is a continuously differentiable function $V(\mathbf{u})$, known as the potential function, satisfying

$$\frac{\partial V(\mathbf{u})}{\partial u_i} = f_i(\mathbf{u}), \quad \text{for all } i \in \mathcal{S}, \text{ and } \mathbf{u} \in \Delta.$$

Assumption 18.2 Fitness functions depend only on strategies on which there is connection, i.e., each node requires only available information given by the graph topology.

Assumption 18.3 The proportion of agents playing the strategies corresponding to intersection nodes are strictly positive for all the time, i.e., $u_i^p > 0$ for all $i \in \mathcal{I}$, and for all $p \in \mathcal{P}$ (i.e., there is not extinction of the intersection population). This also implies that population masses are strictly positive, i.e., $m^p > 0$, for all $p \in \mathcal{P}$, since the population masses are composed of proportion of agents within populations.

Assumption 18.4 The game DDF is a stable game [11], i.e., the Jacobian matrix $D\mathbf{F}(\mathbf{u})$ is negative semi-definite with respect to the tangent space $T\Delta$ (see Definition 18.1).

The features of the potential function $V(\mathbf{u})$ determine whether the full potential game \mathbf{F} is stable, as shown in Lemma 18.1.

Lemma 18.1 *If $V(\mathbf{u})$ is twice continuously differentiable and concave, then the full potential game \mathbf{F} is a stable game.*

The objective for the society is to converge to a Nash equilibrium³ of the game \mathbf{F} denoted by $\mathbf{u}^* \in \Delta$. In order to achieve this objective, there is a game at each

³ $\mathbf{u}^* \in \Delta$ is a Nash equilibrium if each used strategy entails the maximum benefit for the proportion of agents selecting it, i.e., the set of Nash equilibria is given by $\{\mathbf{u}^* \in \Delta : u_i^* > 0 \Rightarrow f_i(\mathbf{u}^*) \geq f_j(\mathbf{u}^*)\}$, for all $i, j \in \mathcal{S}$ [23].

population $p \in \mathcal{P}$ converging to a Nash equilibrium of the game \mathbf{F}^p denoted by $\mathbf{u}^{p*} \in \Delta^p$, and the intersection nodes $i \in \mathcal{I}$ allow a mass interchange among the different populations.

Population Dynamics and Mass Dynamics

A game is solved for each population with constraints given by the population masses m^p , which vary dynamically. Dynamics associated to each population are shown in (18.7a). There are π different dynamics of this form, one for each clique \mathcal{C}^p for all $p \in \mathcal{P}$, i.e.,

$$\dot{u}_i^p = u_i^p (f_i^p - \bar{f}^p - \phi^p), \quad \text{for all } i \in \mathcal{S}^p, \quad (18.7a)$$

$$\phi^p = \beta \left(\frac{1}{m^p} \sum_{j \in \mathcal{S}^p} u_j^p - 1 \right), \quad (18.7b)$$

where β is the convergence factor for the whole system that takes a positive and finite value. Notice that, when $\phi^p = 0$ (i.e., $\mathbf{u}^p \in \Delta^p$), then (18.7a) becomes the classical replicator dynamics equation [27].

On the other hand, there are as many mass dynamics as intersection nodes in the graph, i.e., one for each $i \in \mathcal{I}$. The dynamics for population masses m^p are given by

$$\dot{m}_i^p = m_i^p (u_i - u_i^p), \quad \text{for all } p \in \mathcal{P}_i, \quad (18.8)$$

Equation (18.8) describes the movements of agents among populations through intersection nodes for the case in which there is no social mass constraint [6]. There might be alternative possibilities in the selection of the mass dynamics (18.8). However, the requirements that should be satisfied are as follows: (i) the dynamics satisfy the communication constraints established by the graph \mathcal{G} , and (ii) dynamics converge to the equilibrium point given by $u_i = u_i^p$, for all $p \in \mathcal{P}_i$.

There is a relationship between m_i^p , for all $i \in \mathcal{I}^p$, and the population masses m^p given by

$$m^p = \frac{1}{|\mathcal{I}^p|} \sum_{i \in \mathcal{I}^p} m_i^p, \quad \text{for all } p \in \mathcal{P}. \quad (18.9)$$

For the mass dynamics at intersection nodes in (18.8), the vector of masses and the vector of states associated to an intersection node $i \in \mathcal{I}$ are defined next. The masses vector is denoted by $\mathbf{m}_i = [m_i^{p_1} \dots m_i^{p_{G(i)}}]^\top \in \mathbb{R}^{G(i)}$, where $p_1, \dots, p_{G(i)} \in \mathcal{P}_i$; and the vector of population states is $\mathbf{u}_i = [u_i^{p_1} \dots u_i^{p_{G(i)}}]^\top \in \mathbb{R}^{G(i)}$, where $p_1, \dots, p_{G(i)} \in \mathcal{P}_i$; both vectors \mathbf{m}_i , and \mathbf{u}_i for all $i \in \mathcal{I}$. Notice that, $\mathbf{m}_i \neq m_i$ and $\mathbf{u}_i \neq u_i$.

Finally, the dynamical system can be forced to converge to a Nash equilibrium \mathbf{u}^* such that $\mathbf{F}(\mathbf{u}^*) = \nabla V(\mathbf{u}^*)$ converges to a desired value $f_i(r)$ for an $i \in \mathcal{I}$, where r is a known value (e.g., a reference). Modifying the relationship between the states in (18.4) by adding the reference r , the following new relationship is obtained:

$$u_i = \frac{1}{G(i) + 1} \left(\sum_{p \in \mathcal{P}} u_i^p + r \right),$$

where $u_i^p = 0$, if $i \notin \mathcal{V}^p$. Using this modification, by (18.8), u_i tends to r . This makes \bar{f} to converge to the desired value $f_i(r)$, for only one $i \in \mathcal{I}$.

Optimization Problems

The presented population dynamics with time-variant mass may be implemented to solve different constrained optimization problem forms. First, it is presented a population game without social mass constraint but with the positiveness over the proportion of agents. Afterwards, the population-games approach is presented to solve a constrained optimization problem with several constraints over the proportion of agents.

First, consider optimization problems without social mass constraint. This problem only demands the positiveness of optimization variables. From a mass dynamics perspective, it implies a variation of the social mass arbitrarily. The problem is stated as follows:

$$\begin{aligned} & \underset{\mathbf{u}}{\text{maximize}} && V(\mathbf{u}) \\ & \text{subject to} && \mathbf{u} \in \mathbb{R}_{\geq 0}^n, \end{aligned}$$

where $V : \mathbb{R}_{\geq 0}^n \mapsto \mathbb{R}$, and V is continuously differentiable and concave. Also, it is supposed that the solution point of this problem is an interior point. The solution for the optimization problem with one constraint is found by $\mathbf{F}(\mathbf{u}) = \nabla V(\mathbf{u}) = 0$, since $V(\mathbf{u})$ is concave and by the fact that it is known that the maximum point is an interior point. Therefore, the desired value for the average fitness is $f_i(r) = 0$, and it is enough to find the correct value for reference r and any intersection $i \in \mathcal{I}$.

Secondly, consider optimization problems with multiple constraints over agents proportions. Suppose that there is a strategic interaction with more than one constraint, e.g., different constraints over the proportion of agents. It is desired that the total amount of certain groups of proportions of agents are constant. This problem is stated as

$$\begin{aligned} & \underset{\mathbf{u}}{\text{maximize}} && V(\mathbf{u}) \\ & \text{subject to} && \mathbf{H}\mathbf{u} = \mathbf{h}, \text{ and } \mathbf{u} \in \mathbb{R}_{\geq 0}^n, \end{aligned} \quad (18.10)$$

where $\mathbf{u} \in \mathbb{R}_{\geq 0}^n$, $V : \mathbb{R}_{\geq 0}^n \mapsto \mathbb{R}$, and V is concave and continuously differentiable. Moreover, $\mathbf{H} \in \mathbb{R}^{L \times n}$ since there are L constraints and n decision variables, and $\mathbf{h} \in \mathbb{R}^L$. For this optimization problem, $\boldsymbol{\mu}$ is the Lagrange multiplier vector. The Lagrange function $l : \mathbb{R}^n \times \mathbb{R}^L \mapsto \mathbb{R}$ is

$$l(\mathbf{u}, \boldsymbol{\mu}) = V(\mathbf{u}) + \boldsymbol{\mu}^\top (\mathbf{H}\mathbf{u} - \mathbf{h}). \quad (18.11)$$

Moreover, $\nabla_{\mathbf{u}}l(\mathbf{u}, \boldsymbol{\mu}) = \nabla f(\mathbf{u}) + \mathbf{H}^\top \boldsymbol{\mu}$, and $-\nabla_{\boldsymbol{\mu}}l(\mathbf{u}, \boldsymbol{\mu}) = -\mathbf{H}\mathbf{u} + \mathbf{h}$. The Lagrange condition is used to find possible extreme points in the objective function, in which $\nabla_{\mathbf{u}}l(\mathbf{u}, \boldsymbol{\mu}) = \mathbf{0}$, $\nabla_{\boldsymbol{\mu}}l(\mathbf{u}, \boldsymbol{\mu}) = \mathbf{0}$ [8].

Consequently, fitness functions for each node are chosen to be defined as $\mathbf{F}(\mathbf{u}) = \nabla_{\mathbf{u}}l(\mathbf{u}, \boldsymbol{\mu})$, and $\mathbf{F}(\boldsymbol{\mu}) = \nabla_{\boldsymbol{\mu}}l(\mathbf{u}, \boldsymbol{\mu})$. This problem is solved by using a reference r as it was explained in Sect. 18.3.2 in order to force a convergence value for the fitness functions associated to the social states and the Lagrange multipliers. In order to use the population and the mass dynamics, it is necessary that the games are stable according to Assumption 18.3.

Lemma 18.2 *If $V(\mathbf{u})$ is twice continuously differentiable and concave, and the constraints have the form $\mathbf{H}\mathbf{u} = \mathbf{h}$, then the games $\mathbf{F}(\mathbf{u}) = \nabla_{\mathbf{u}}l(\mathbf{u}, \boldsymbol{\mu})$ and $\mathbf{F}(\boldsymbol{\mu}) = \nabla_{\boldsymbol{\mu}}l(\mathbf{u}, \boldsymbol{\mu})$ are stable.*

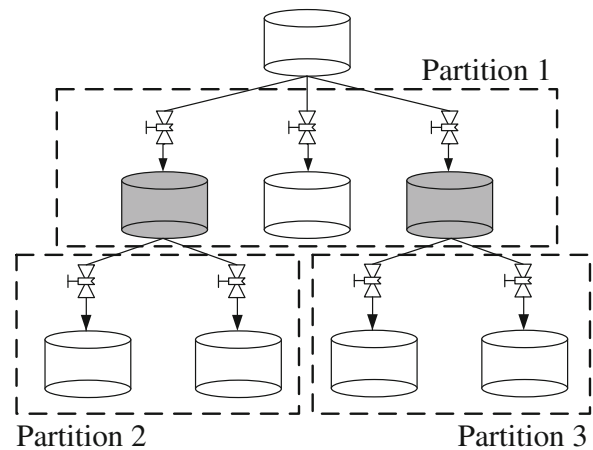
18.4 Simulations and Results

18.4.1 Case Study: First Data-Driven Perspective

In the design of the proposed decentralized controller, it is necessary to make a partitioning of the DWTN into different subsystems. Each subsystem must correspond to a case of flow divergence (i.e., each subsystem must be of the form shown in Fig. 18.1). In order to clarify the partitioning process in a typical branched DWTN, an arbitrary DWTN is presented in Fig. 18.3. At this general example, it is possible to identify that the whole system is composed of three partitions or subsystems.

When performing the partitioning, it is possible to find some tanks that are a source and also a receptor for different subsystems in the DWTN (this is typical when the topology is *branched*). For instance, in the partitioning presented in Fig. 18.3, the grey tanks are receptors for the partition 1, and source tanks for the partitions 2, and 3.

Fig. 18.3 Partitions over a branched topology. Some tanks are source and receptor in different partitions (*gray tanks*)



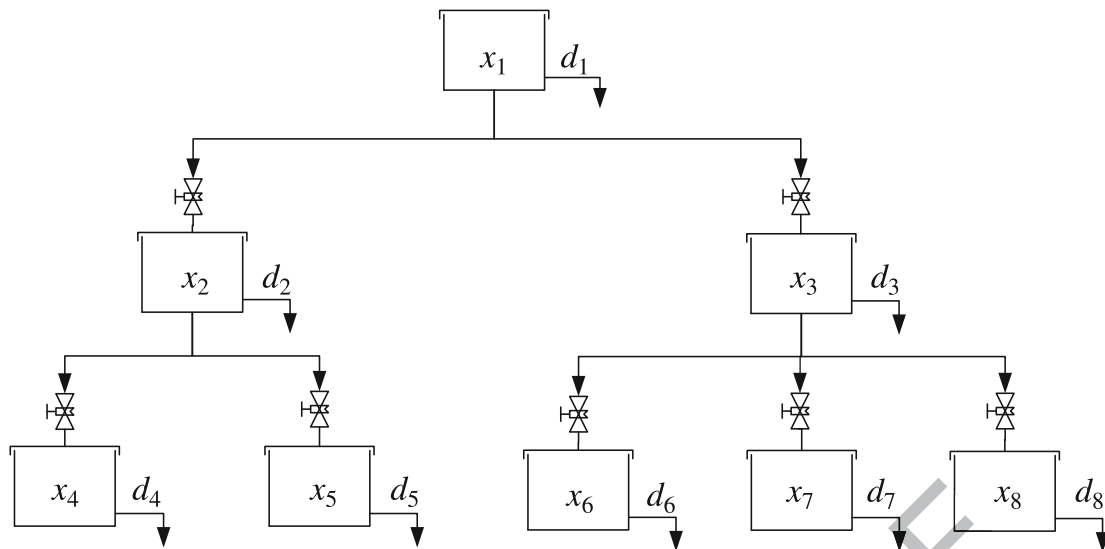


Fig. 18.4 Case study with eight tanks in a branched DWTN

Table 18.2 Maximum volumes and scale factors of the tanks in the DWTN

Tank i	x_i^{\max} (m ³)	K_i (1/ms)
1	2.0	0.123
2	1.1	0.160
3	2.0	0.326
4	0.5	0.599
5	2.6	0.660
6	0.2	0.632
7	2.0	0.255
8	3.5	0.427

A DWTN composed by eight tanks is controlled (see Fig. 18.4), for an scenario in which shortages are produced due to the fact that the network is only operating with water stored in the main upstream tank. The system is a branched DWTN whose topology is mainly divergent, so it can be partitioned in three main subsystems; all independently controlled by a distributed replicator-dynamics-based controller. The maximum storage capacity and the scale factors of each tank are presented in Table 18.2. Since the system is branched and the divergence topology prevails, it is possible to divide the system into three partitions, as it was described before. The first one is composed by tanks 2 and 3, the second by tanks 4 and 5 and the third by tanks 6, 7 and 8. Each partition receives the flow from a source tank, which is distributed in different proportions, depending on the setting of the input valves of each tank of the partition.

Each tank attends a different demand pattern along the day denoted by d_i . The tanks with volumes x_5 and x_8 supply a constant demand pattern of 4.5×10^{-3} l/s, while the others, denominated as inactive tanks (i.e., tanks 2, 3, 4, 6 and 7) are just operating to store water, not attending any demand pattern. When there is not

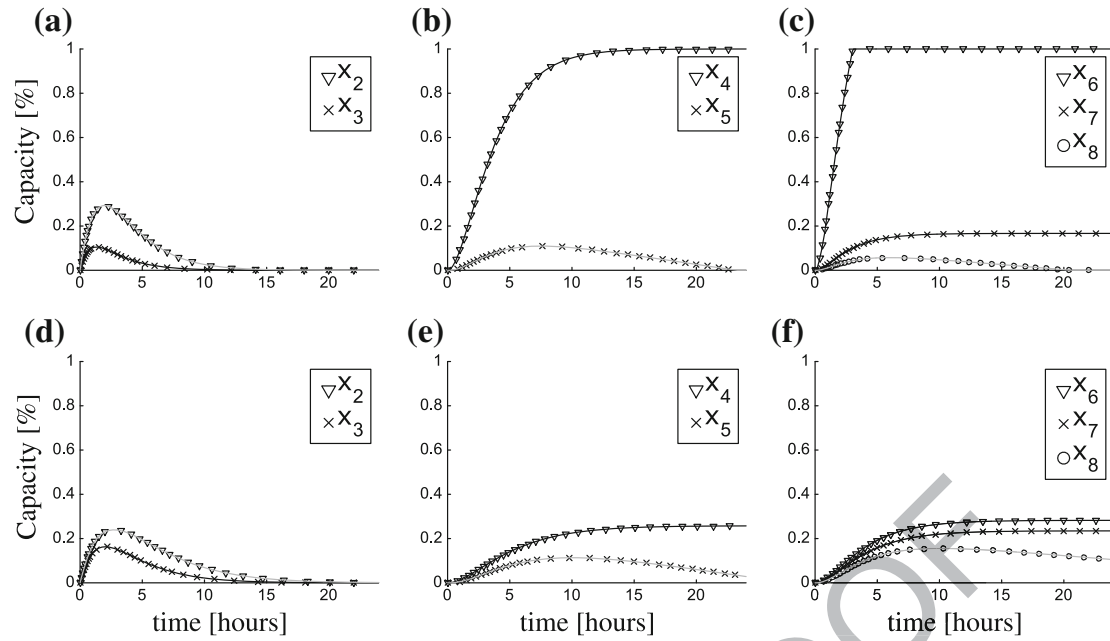


Fig. 18.5 Evolution of the used capacity in storage tanks; **a, b, c** capacity of tanks when no control strategy is applied; and **d, e, f** capacity of tanks when the evolutionary-game-based strategy with the replicator dynamics is applied

a control strategy, the flow is divided equally, and shortage of 26 m^3 is produced because the distribution of flows is inefficient, as shown in Figs. 18.5a, 18.5b and 18.5c.

When the control strategy is applied, then the priority is given to the tanks that supply the demand, and inactive tanks become less filled up since they are not attending any demand pattern. Thereby, no shortages are produced, the demand is fully supplied and the distribution of flows is more efficient, in comparison to the case with no control. This is because all the tanks keep some volume stored on them at the end of the day, while in the other case, tanks 5 and 8 are completely empty.

It has been shown that the proposed decentralized population dynamics-based control is efficient in terms of a better distribution of drinking water throughout the DWTN, avoiding shortages. The partitioning proposed methodology allows to design the decentralized controller by using different local controllers with a lower computational burden with respect to a centralized controller.

18.4.2 Case Study: Second Data-Driven Perspective

Consider the case study presented in Fig. 18.6, which corresponds with the aggregate model of the Barcelona drinking water network presented in Fig. 2.2. For this system, consider $\tilde{\mathbf{x}} = [\tilde{x}_1 \ \tilde{x}_2 \ \dots \ \tilde{x}_{61}]^\top$, $\tilde{\mathbf{x}}_s = [\tilde{x}_{s,1} \ \tilde{x}_{s,2} \ \dots \ \tilde{x}_{s,61}]^\top$ and $\mathbf{u} = [u_1 \ u_2 \ \dots \ u_{61}]^\top$ according to the explanation presented in Sect. 18.2.2.

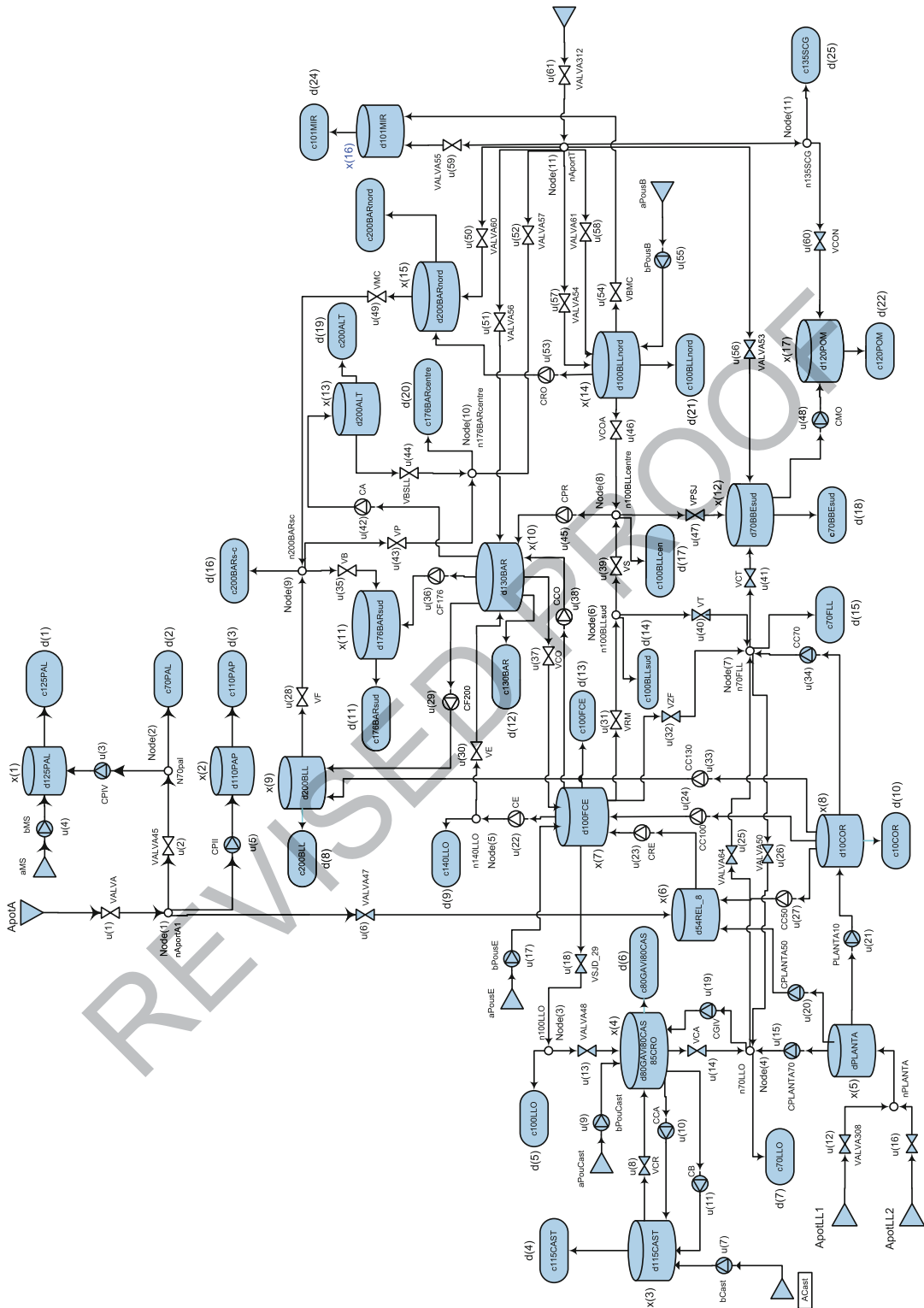


Fig. 18.6 Aggregate model of the Barcelona DWTN (BDWTN) comprised by 17 states, 61 control actions, 25 demands and 11 mass balance nodes

In the control design, the first step is the determination of cliques within the system, i.e., to make a partitioning of the system. The aforementioned partition process of the BDWTN is a problem already studied in [18]. For the BDWTN control problem, the proposed partitioning is determined based on the system mass balance constraints. Lagrange-multiplier vertices are connected to decision variables vertices from which information is needed in order to compute the fitness functions $\mathbf{F}(\mu)$. As a criterion for performing the partitioning, it is desired that all the Lagrange multipliers, and the nodes connected with them, belong to the same clique. In order to formalize this partitioning criterion, let \mathcal{H}_j be the set of all the nodes that are involved in the j th equality constraint of the form (18.10), where $j = 1, \dots, L$, e.g., for the BDWTN system, $\mathcal{H}_1 = \{1, 2, 5, 6\}$, and $\mathcal{H}_2 = \{2, 3\}$. Furthermore, we consider two sets of nodes for mass balance constraints \mathcal{H}_i , and \mathcal{H}_j . If $\mathcal{H}_i \cap \mathcal{H}_j \neq \emptyset$, then all the nodes $\mathcal{H}_i \cup \mathcal{H}_j$ should belong to the same clique.

Based on this idea, it is possible to determine the vertices (strategies) that should belong to the same clique (population). As an example, consider the set of nodes associated to the constraint given by mass balance node 9, i.e., $\mathcal{H}_9 = \{28, 35, 43, 49\}$, and the set of nodes corresponding to the mass balance constraint 10, i.e., $\mathcal{H}_{10} = \{43, 44, 52\}$. There is a common vertex given by $\mathcal{H}_9 \cap \mathcal{H}_{10} = \{43\}$. Now, considering the constraint corresponding to the mass balance node 11, i.e., $\mathcal{H}_{11} = \{50, 51, 52, 56, 57, 58, 59, 60, 61\}$, then it is obtained that $\mathcal{H}_{10} \cap \mathcal{H}_{11} = \{52\}$. Consequently, all the nodes $\mathcal{H}_9 \cup \mathcal{H}_{10} \cup \mathcal{H}_{11}$ should belong to the same clique.

On the other hand, there are some vertices that are not associated to any constraint, e.g., the node 4 associated to the decision variable x_4 , then $4 \notin \mathcal{H}_j$ for all $j = 1, \dots, 11$. In these cases, vertices are assigned to the closest clique. Cliques are presented in Fig. 18.7, and the nodes of each clique are shown in Table 18.3. Notice that $\{\mathcal{H}_1 \cup \mathcal{H}_2 \cup \mathcal{H}_3 \cup \mathcal{H}_5\} \in \mathcal{V}^1$, $\{\mathcal{H}_4 \cup \mathcal{H}_6 \cup \mathcal{H}_7 \cup \mathcal{H}_8\} \in \mathcal{V}^2$, and $\{\mathcal{H}_9 \cup \mathcal{H}_{10} \cup \mathcal{H}_{11}\} \in \mathcal{V}^3$.

Once the partitioning is performed, the optimization problem (18.1) is stated of the form (18.10) by adding slack variables, which may be solved by using the population and mass dynamics. In this case, the society is composed of three population (cliques). In order to analyze the performance of the data-driven controller, the obtained results are compared to a centralized MPC controller. Figure 18.8 presents the evolution of three volume tanks (i.e., x_1 , x_{12} , and x_{14}), and three control inputs (i.e., u_{18} , u_{32} , and u_{40}) for both centralized MPC controller and data-driven controller based on population dynamics. In Figs. 18.8a, 18.8b and 18.8c show that, with the centralized MPC controller, the tanks are maintained with more volumes with respect to the data-driven controller based on population dynamics. This better performance of the centralized MPC controller is obtained due to the fact it disposes of the system model in comparison to the data-driven control approach. Moreover, Figs. 18.8d, 18.8e and 18.8f show the similar performance of the control inputs for both controller. This close behaviour is obtained because of the constraints, which are taken into account for both control approaches.

Table 18.4 shows the comparison of the economical costs obtained with the centralized MPC strategy and the data-driven population-games-based control approach. The results exhibit lower energy costs associated to the control inputs with the

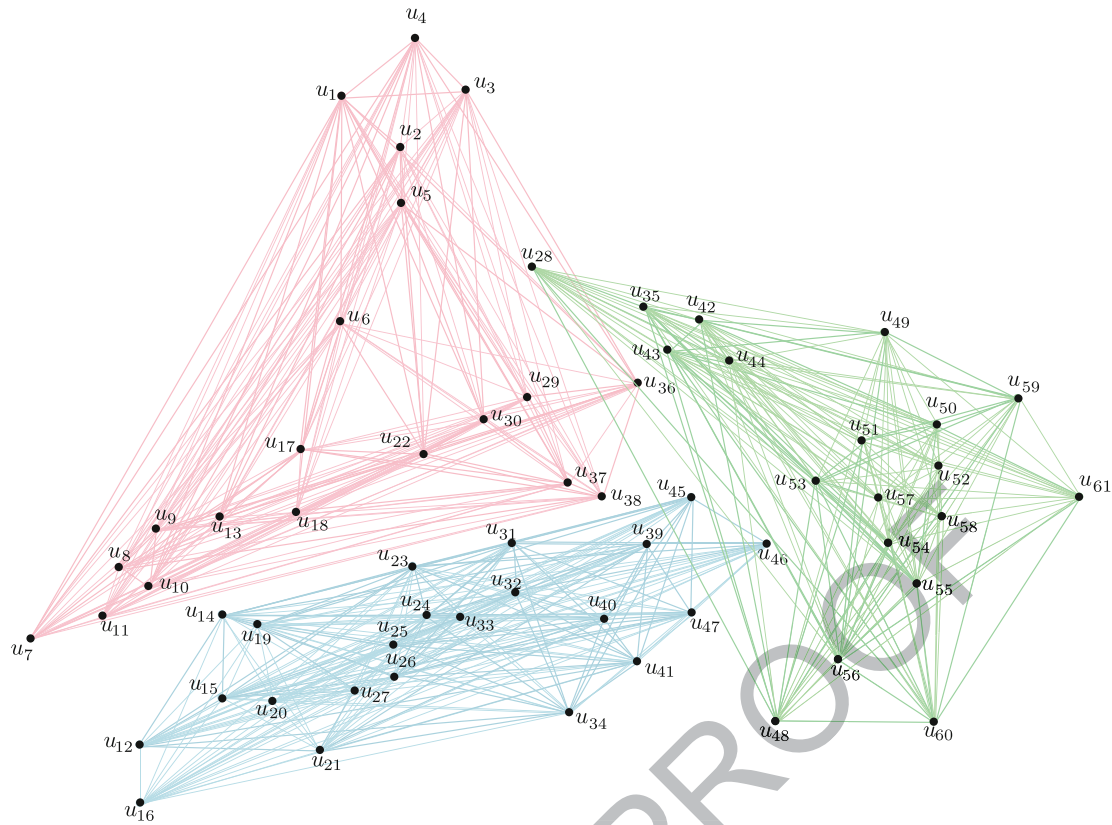


Fig. 18.7 Partitioning of the BDWTN into three cliques (see Table 18.3)

data-driven approach. However, since the MPC controller disposes of the model system to generate a prediction, the centralized MPC approach minimizes more the overall costs. In contrast, even though the minimization of costs, the data-driven control scheme is non-centralized, reducing the amount of required communication links in order to compute the final control inputs.

Table 18.3 Partitioning of the network into the three resultant cliques

Clique	Vertices u	Involved states x
1	1, 2, 3, 4, 5, 6, 7, 8, 9, 10, 11, 13, 17, 18, 22, 29, 30, 36, 37, 38	1, 2, 3, 4, 6, 7, 9, 10, 11
2	12, 14, 15, 16, 19, 20, 21, 23, 24, 25, 26, 27, 31, 32, 33, 34, 39, 40, 41, 45, 46, 47	4, 5, 6, 7, 8, 9, 10, 12, 14
3	28, 35, 42, 43, 44, 48, 49, 50, 51, 52, 53, 54, 55, 56, 57, 58, 59, 60, 61	9, 10, 11, 12, 13, 14, 15, 16, 17

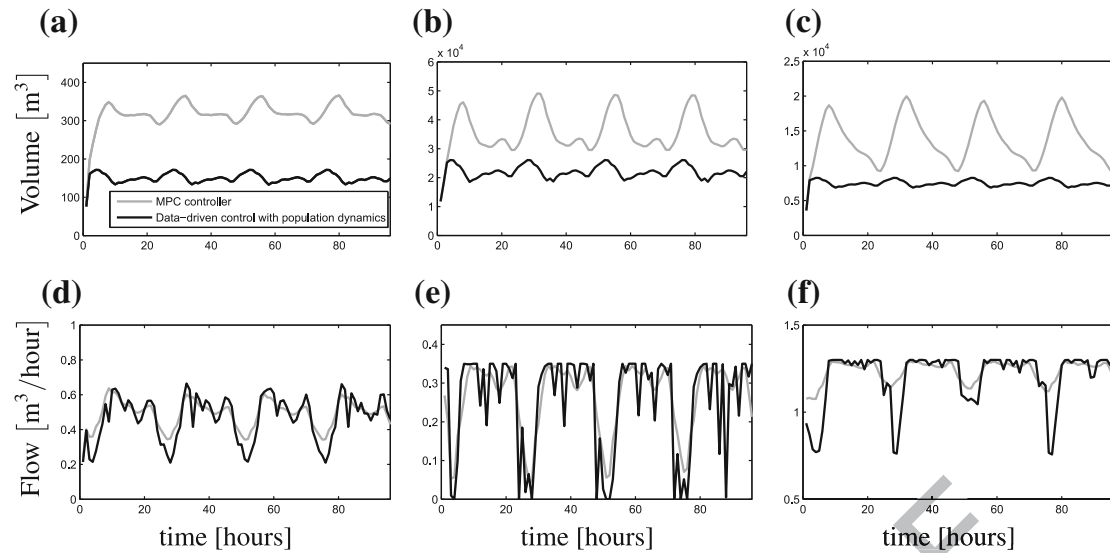


Fig. 18.8 Evolution of volumes **a** 1, **b** 12, and **c** 14. Evolution of control inputs **d** 18, **e** 32, and **f** 40

Table 18.4 Discrimination of economical costs for different control strategies

Day	Total cost in economical units (e.u.)			
	Population dynamics approach		Model predictive control	
	Data-driven controller		Model-based controller	
	Water	Energy	Water	Energy
1	45484.48	18409.34	37915.28	22096.12
2	41384.76	18131.81	28352.38	22235.15
3	40022.43	18791.73	28400.39	22288.11
4	40389.76	18387.35	28330.14	22219.59
Sum	167281.43	73720.23	122998.21	88838.97
Overall costs	241001.66		211837.17	

18.5 Conclusions

Two data-driven non-centralized control strategies to manage water flows among drinking-water networks have been presented. The proposed controllers are based on population games and have been designed using the distributed replicator dynamics and a modification of the population dynamics incorporating mass dynamics. Additionally, two partitioning approaches have been introduced in order to divide the typical centralized control problem into several subsystems. The partitioning of the system allows to reduce the computational burden required to manage the flows among the system. In the first population-games approach, the partitioning implies a decentralized control scheme since the local controllers do not communicate to each other. On the other hand, the partitioning in the second population-games implies a

distributed control scheme since there is overlapping among the resulting subsystems. Both techniques have been tested using two different case studies.

References

1. Arslan G, Shamma J (2004) Distributed convergence to Nash equilibria with local utility measurements. In: Proceedings of the 43rd IEEE Conference on Decision and Control (CDC), Atlantis, Paradise Island, Bahamas, pp 1538–1543
2. Barreiro-Gomez J, Obando G, Quijano N (2016) Distributed population dynamics: optimization and control applications. *Trans Syst Man Cybern* 99:1–11
3. Barreiro-Gomez J, Obando G, Riaño Briceño G, Quijano N, Ocampo-Martinez C (2015) Decentralized control for urban drainage systems via population dynamics: Bogotá case study. In: Proceedings of the European Control Conference (ECC), Linz, Austria
4. Barreiro-Gomez J, Quijano N, Ocampo-Martinez C (2014) Constrained distributed optimization based on population dynamics. In: Proceedings of the 53rd IEEE Conference on Decision and Control (CDC), Los Angeles, California, USA, pp 4260–4265
5. Barreiro-Gomez J, Quijano N, Ocampo-Martinez C (2014) Distributed control of drinking water networks using population dynamics: Barcelona case study. In: Proceedings of the 53rd IEEE Conference on Decision and Control (CDC), Los Angeles, California, USA, pp 3216–3221
6. Barreiro-Gomez J, Quijano N, Ocampo-Martinez C (2016) Constrained distributed optimization: a population dynamics approach. *Automatica* 69:101–116
7. Bomze IM, Pelillo M, Stix V (2000) Approximating the maximum weight clique using replicator dynamics. *IEEE Trans Neural Netw Learn Syst* 11(6):1228–1241
8. Chong EKP, Zak SH (2011) An introduction to optimization. Series in discrete mathematics and optimization. Wiley
9. Grosso JM, Ocampo-Martinez C, Puig V, Limon D, Pereira M (2014) Economic MPC for the management of drinking water networks. In: European Control Conference (ECC), Strasbourg, France, pp 790–795
10. Grundmann Jens, Schütze Niels, Schmitz Gerd, Al-Shaqsi Saif (2012) Towards an integrated arid zone water management using simulation-based optimization. *Environ Earth Sci* 65(5):1381–1394
11. Hofbauer J, Sandholm WH (2009) Stable games and their dynamics. *J Econ Theory* 144(4):1665–1693
12. Johnston HC (1976) Cliques of a graph-variations on the Bron-Kerbosch algorithm. *Int J Parallel Prog* 5(3):209–238
13. Kalbus E, Kalbacher T, Kolditz O, Krüger E, Seegert J, Röstel G, Teutsch G, Borchardt D, Krebs P (2012) Integrated water resources management under different hydrological, climatic and socio-economic conditions. *Environ Earth Sci* 65(5):1363–1366
14. Lasaulce S, Tembine H (2011) Game theory and learning for wireless networks: fundamentals and applications. Academic Press
15. Marden J (2012) State based potential games. *Automatica* 48:3075–3088
16. Marden J, Shamma J (2015) Game theory and distributed control. In: Handbook of game theory with economic applications, pp 861–899. Elsevier
17. Marden JR, Shamma JS (2014) Game theory and distributed control. In: Handbook of Game Theory, vol 4, pp 861–899
18. Ocampo-Martinez C, Bovo S, Puig V (2011) Partitioning approach oriented to the decentralised predictive control of large-scale systems. *J Process Control* 21:775–786
19. Price RK, Vojinović Z (2011) Urban hydroinformatics: data, models, and decision support for integrated urban water management. IWA Publishing

20. Ramirez-Llanos E, Quijano N (2010) A population dynamics approach for the water distribution problem. *Int J Control* 83(9):1947–1964
21. Riaño-Briceño G, Barreiro-Gomez J, Ramirez-Jaime A, Quijano N, Ocampo-Martinez C (2016) MatSWMM—An open-source toolbox for designing real-time control of urban drainage systems. *Environ Model Softw* 83:143–154
22. Sandholm WH, Dokumaci E, Lahkar R (2008) The projection dynamic and the replicator dynamic. *Games Econ Behav* 64(2):666–683
23. Sandholm WH (2010) *Population games and evolutionary dynamics*. MIT Press, Cambridge, Mass
24. Tembine H, Altman E, El-Azouzi R, Hayel Y (2010) Evolutionary games in wireless networks. *IEEE Trans Syst Man Cybern Part B Cybern* 40(3):634–646
25. UNICEF (2015) *Progress on sanitation and drinking water update and MDG assessment*. World Health Organization, Geneva
26. Wang Y, Ocampo-Martinez C, Puig V (2015) Robust model predictive control based on Gaussian processes: application to drinking water networks. In: *Proceedings of the European Control Conference (ECC)*, Linz, Austria
27. Weibull JW (1997) *Evolutionary game theory*. The MIT Press, London, England

REVISED PROOF